The residual oil saturation determination for Steam Assisted Gravity Drainage (SAGD) and Solvent-SAGD

Taniya Kar [a], Cesar Ovalles [b], Estrella Rogel [b], Janie Vien [b], Berna Hascakir [a,*]

[a] Texas A&M University Petroleum Engineering Department, College Station, TX 77843-3116, United States
[b] Chevron ETC, 100 Chevron Way, Richmond, CA 94802, United States

ABSTRACT

The residual oil saturation determination is critical for the performance evaluation of any Enhance Oil Recovery (EOR) methods. The existing residual oil saturation determination methods are mainly based on solvent extraction. However, because the quality of the extracted residual oil and the remaining spent rock samples have not been examined before, this study investigates the accuracy of two commonly used solvent extraction methods for the residual oil saturation determination extracted from the spent rock samples of Steam Assisted Gravity Drainage (SAGD) and Solvent-SAGD. The results of the commonly used solvent extraction methods were compared with a new thermal method. It has been found that the thermal method provides more accurate results than solvent extraction method because the reservoir clays interact with residual oil and solvent methods cannot successfully separate the residual oil from reservoir rock. Therefore, a significant amount of clay is detected in the extracted residual oil through solvent extraction. Moreover, this study reveals that among the saturates, aromatics, resins, and asphaltenes fractions of residual oil, the aromatics fraction is responsible for the clay–asphaltene interaction and the resins content reduces this interaction. Because the solvents used to separate residual oil from rock samples are in general strong aromatic solvents, the existing solvent extraction methods fail to determine the residual oil saturation amount accurately.

© 2016 Published by Elsevier Ltd.

1. Introduction

The target of any Enhanced Oil Recovery (EOR) methods is to reduce the residual oil saturation that can be achieved by overcoming the surface forces between solid-oil and oil–water interfaces [1,2]. Hence, the residual oil saturation determination is required to evaluate the performance of any recovery methods. The residual oil saturation determination is not easy. The advantageous and disadvantageous of existing residual oil saturation determination methods were summarized before [3,4]. In these reviews, it has been reported that the most accurate methods to determine residual oil are either very challenging or too expensive. Easy to apply and cost-effective techniques are reported as misleading. Among the earliest techniques to determine residual oil saturation are core flood experiments [5,6]. In laboratory waterflooding techniques, the obtained values of residual oil saturation in restored cores vary compared with those with original (without exposure to the atmosphere or cleaning) reservoir cores [7]. More recently, Nuclear Magnetic Resonance (NMR) relaxometry measurements have been used to determine residual oil saturation in terms of distribution of oil in the pores of varying sizes in waterflooding applied to tight oil formations [8]. The limitations of this technique are that it cannot quantify capillary end effects [9]. Even though, wettability information is available in the literature for waterflooding, this information is mostly for the conventional reservoirs, and it is not sufficient to be adapted for the estimation of the performance of the steam injection processes into unconventional reservoirs [10,11]. Moreover, the residual oil saturation dynamically changes due to water interaction with rock and reservoir fluids at varying temperature values [12–15]. The residual oil saturation variation due to temperature changes is more pronounced for bitumen and heavy oils than the lighter ones because wettability is also affected by the fluid density and the polarity of oil components [16]. Bitumen is known to contain high amounts of polar components such as asphaltenes and resins and also, water is a polar molecule [17,18]. Hence, any estimation of wettability alteration during steam injection for a bitumen reservoir by using a light oil with less or no polar components would be misleading.

For high asphaltene content reservoir, commonly, residual oil saturation can be determined using solvent extraction, by

* Corresponding author.
   E-mail addresses: hascakir@tamu.edu, hascakir@gmail.com (B. Hascakir).

Nomenclature

ASTM	American Society for Testing and Materials	ELSD	Evaporating Light Scattering Detector
CHN	carbon, hydrogen, nitrogen	EOR	Enhanced Oil Recovery
C6	hexane	ES-SAGD	Expanding Solvent Steam Assisted Gravity Drainage
CWE	cold water equivalent measured at atmospheric conditions	FTIR	Fourier Transform Infrared Spectroscopy
		NMR	Nuclear Magnetic Resonance
DAO	deasphalted oil	S1	Solvent 1-mixture of 90% dichloromethane + 10% methanol
DCM	dichloromethane		
E1	SAGD	S2	Solvent 2-Toluene
E2	solvent SAGD with n-hexane	SAGD	Steam Assisted Gravity Drainage
E3	solvent SAGD with co-injection of n-hexane and toluene	SARA	Saturates, aromatics, resins, asphaltenes
E4	solvent SAGD with cyclic injection of n-hexane and toluene	SEM	Scanning Electron Microscopy
		S_{oi}	initial oil saturation
E5	solvent SAGD with co-injection of n-hexane and cyclohexane	S_{or}	residual oil saturation
		TGA	thermogravimetric Analysis
EDS	Energy Dispersive Spectroscopy	Th	thermal method

employing a powerful solvent capable of dissolving even the heavier fractions of the crude oil, like resins and asphaltenes. Examples of these solvents are toluene [19] and dichloromethane (DCM). The drawback of this method is that some reservoir fines (sand and clay particles) can infiltrate into the oil extracted from the spent rock by these solvents, which can cause errors in the measurement [20–23].

Steam-Assisted Gravity Drainage (SAGD) is one of the most effective bitumen extraction methods [24,25]. To enhance the process performance of SAGD and to reduce several drawbacks of the process due to steam generation, the application of Solvent-SAGD processes became more popular [26–29]. However, the residual oil saturation determination for SAGD and Solvent-SAGD has not been studied extensively before. But, it is known that the steam–solvent–bitumen interactions become complicated in Solvent-SAGD processes due to the solubility of polar oil components in various solvents [23,30]. Asphaltenes and resins are the polar components of bitumen and bitumen has high asphaltene content. Asphaltenes are insoluble in paraffinic hydrocarbons, but are soluble in aromatic solvents [17]. Depending on the solubility of asphaltenes in solvents, the residual oil saturation will be altered during Solvent-SAGD, due to the precipitation of heavier fractions mainly. The mutual interactions of oil components, i.e., saturates, aromatics, resins, and asphaltenes (SARA), on wettability have been analyzed before through SARA analysis [31]. However, the residual oil saturation alteration has not been studied before for SAGD and Solvent-SAGD and how the reservoir fines will contribute toward this alteration is not very well known.

Therefore, this research aims to investigate the accurate determination of the residual oil saturation for SAGD and Solvent-SAGD. The role of reservoir clays on residual oil saturation determination is further examined and the role of SARA fractions on asphaltenes stability is discussed.

2. Experimental procedure

One SAGD and four Solvent-SAGD experiments have been conducted previously on a Canadian bitumen (8.8 °API). A detailed description of the experiments and solvent selection and injection strategies can be found in previously published works [26,28,30]. However, a brief description of the experimental procedure for SAGD and Solvent-SAGD is still presented below. A two-dimensional, stainless steel core holder was used to conduct the experiments. The reservoir rock was prepared by mixing 85 wt% sand with 15 wt% clay (kaolinite and illite mixture). 32% porosity was filled with 84% bitumen and 16% distilled water. The constant,

18 mL/min, cold water injection rate to generate steam at 165 °C and 75 psig back pressure was maintained for each experiment. Three different solvents and two different injection strategies were implemented in Solvent-SAGD experiments. The n-hexane, cyclohexane, and toluene have been used at 2 mL/min injection rate. The solvent selection was made according to their solubility in asphaltenes and their vapor pressures at steam temperature and experimental pressure conditions; n-hexane and cyclohexane are in vapor form at the experimental conditions (165 °C and 75 psig), but n-hexane is insoluble, and cyclohexane is partially soluble in asphaltenes. Toluene, on the other hand, is in liquid form at experimental conditions and completely soluble in asphaltenes [17,32].

E1 was the base SAGD experiment in which no solvent was used, and this experiment took 12 h. E2 through E5 were the Solvent-SAGD experiments and all Solvent-SAGD experiments except E5 took 9 h. E5 had to be terminated by the end of 2.8-h experiment time, due to unexpected plug occurred in production lines [28]. In E2, 2 mL/min n-hexane was coinjected with 18 mL CWE/min steam; in E3, 1 mL/min n-hexane and 1 mL/min toluene mixture was coinjected with 18 mL CWE/min steam; in E4, either 2 mL/min n-hexane or 2 mL/min toluene with one-hour cycles was coinjected with 18 mL CWE/min steam; and in E5, 1 mL/min n-hexane and 1 mL/min cyclohexane mixture was coinjected with 18 mL CWE/min steam [26,28].

Because the aim of this study is to investigate the residual oil saturation variation for SAGD and Solvent-SAGD, this section will concentrate more on the experimental procedure to analyze the spent rock samples.

After the experiments, visual analysis of the spent rock samples was accomplished. Accordingly, samples have been divided into two zones; steam chamber and steam chamber edge regions. Fig. 1 shows the sample locations on postmortem pictures that were examined for residual oil saturation. These locations were selected based on visual differences in color of the samples and the temperature profiles given in previously published works [26,28]. The blue circles indicate the sample locations collected inside steam chamber region. These regions have a lighter color with less consolidated texture, more importantly, the temperature in these regions were measured at 165 °C by the end of each experiment at 75 psig [26,28]. The yellow circles indicate the sample locations collected at steam chamber edge. These regions have a darker color with consolidated texture. The temperature of those zones were reported at around 155 °C at 75 psig [26,28]. While the temperature and pressure conditions in blue circled regions provide water in 100% vapor phase, in yellow circled regions provide water in the liquid phase.
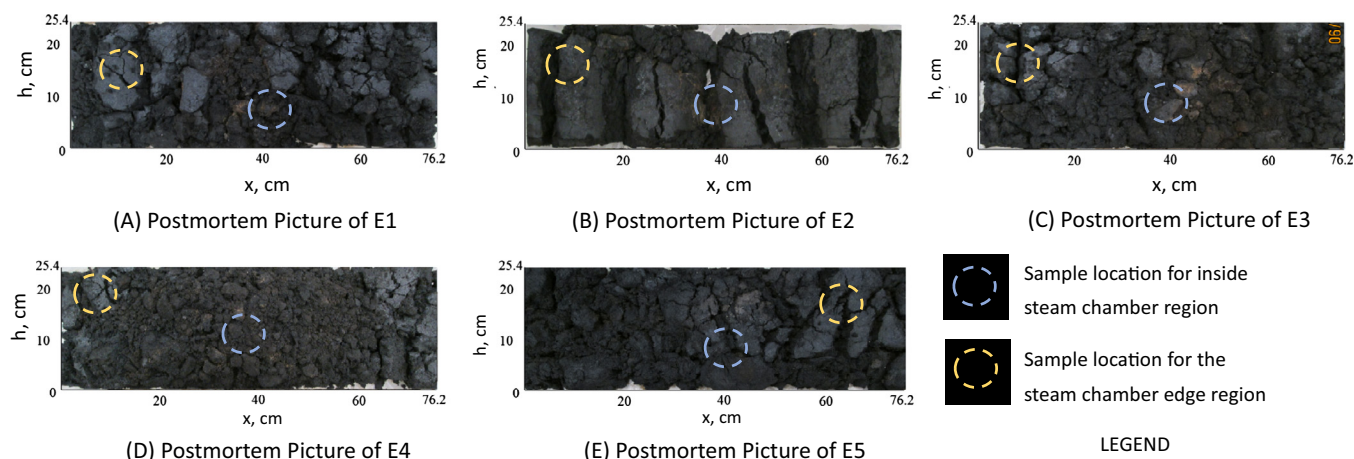
Fig. 1. Sample locations for residual oil saturation determination (injection well location is *x* = 38.1 cm and *h* = 7.5 cm, production well location is *x* = 38.1 cm and *h* = 2.5 cm).

After deciding sample locations, the residual oil saturations determinations were carried out on the spent rock samples that the residual water and solvents were removed previously in a vacuumed environment [28]. The residual oil saturations were determined using two methods (solvent and thermal extraction) on the samples collected from the designated regions given in Fig. 1. For solvent extraction, two different solvents were used; a mixture of 90% dichloromethane (DCM) and 10% methanol (S1) [33] and toluene (S2) [19]. The thermal method (Th) was carried out by Thermogravimetric Analyzer (TGA). During TGA experiments, the spent rock samples were heated under air injection at constant 10 °C/min heating rate till reaching 900 °C. The weight loss curve obtained with TGA analysis were used to calculate the total weight of residual oil on rock samples. For reference, the similar TGA experiment was performed on the original oil-sand mixture. This control experiment was conducted to determine the temperature necessary to decompose all bitumen sample from sand, which corresponds 84 volume percent of 8.8° API gravity bitumen. Another reference measurement for TGA analyses was achieved on original bitumen sample to determine the optimum heating rate. 5, 10, and 20 °C/min heating rates were tested on the original bitumen, zero weight loss was observed for all heating rates at around 550–650 °C. To save time and to protect TGA device, 10 °C/min was selected to implement for all spent rock samples (Table A-1-A).

The residual oil obtained from each zone (Fig. 1) has been subjected to SARA analysis using the ASTM D2007-11 method [34]. This ASTM method starts with the separation of asphaltenes by using n-pentane. Another ASTM method (ASTM D6560-12) which uses n-heptane was also used to separate asphaltenes from the residual oil samples [35]. Therefore, in this study, both n-pentane and n-heptane insoluble asphaltenes originated from the residual oil samples of SAGD and Solvent-SAGD were investigated. The SARA analyses were conducted only by following ASTM D2007-11 method.

The residual oil samples and SARA fractions were further analyzed by Fourier Transform Infrared (FTIR) Spectroscopy to observe the existence of water and clays on spent rock surfaces and on their SARA fractions. In bulk residual oil samples, significant clay presence was observed through FTIR analyses. Moreover, lump formation was observed on the reservoir rock samples washed with solvents for residual oil saturation determination. The Scanning Electron Microscopy and Energy Dispersive Spectroscopy (SEM–EDS) analyses of those lumps provided high carbon signatures that were the indication of hydrocarbon trapping in the reservoir rock [36]. Because n-heptane insoluble asphaltenes were consumed during the determination of n-heptane asphaltenes; the asphaltene–clay separation was accomplished for only n-pentane insoluble asphaltenes by combining both filtration and solvent extraction techniques [19,30]. The size of the filter paper for filtration was selected less than the clay particle size (2.3 μm: [23]), and the asphaltene samples were washed through the filter paper by using toluene. The same procedure was applied to determine the amount of clay in bulk residual oil samples.

N-heptane asphaltenes were used to determine the solubility profiles. The definition and use of solubility profiles are provided in the following section, this section will only describe the experimental procedure for the solubility profile determination. First, n-heptane asphaltenes were quantified using an Evaporative Light Scattering Detector (ELSD) and an HPLC system consisting of a HP Series 1100 chromatograph and an Alltech ELSD 2000 detector [37]. The precipitated n-heptane asphaltenes in the column of the ELSD-HPLC system were washed with solvents gradually; first with pure n-heptane, then, with 90/10 methylene chloride/methanol, and finally with 100% methanol. The procedure redissolves the asphaltenes gradually from the EDA (low solubility parameter: easy to dissolve) of the DDA (high solubility parameter: difficult to dissolve). Based on the ELSD detector, a curve is generated that is related to the solubility properties of the asphaltenes and can be quantified to reflect the tendency of the sample toward asphaltene precipitation [33].

3. Experimental results

3.1. Characterization of original bitumen

This section will summarize first the characterization studies on the original bitumen and original bitumen asphaltenes. Two methods were used to separate asphaltenes; ASTM D2007-11 and ASTM D6560-12. The n-pentane insoluble asphaltene content of the original bitumen sample was 34.3 wt% [34] and the n-heptane insoluble asphaltene content of the original bitumen sample was 27.79 wt% [35]. Fig. 2 shows the metal and sulfur content of the original bitumen and the n-pentane insoluble asphaltenes. Note that because of the methodology used to determine n-heptane insoluble asphaltenes, all asphaltenes were consumed during the determination of the n-heptane asphaltenes and the solubility profiles. Hence, the n-heptane insoluble asphaltenes could not be subjected to elemental analyses.

As expected, asphaltenes are rich in metals and sulfur. Metals like iron and aluminum have been reported before for asphaltenes as well as non-metals like chlorine [38]. How metals are present in the crude oil and associated with asphaltenes is still a matter of
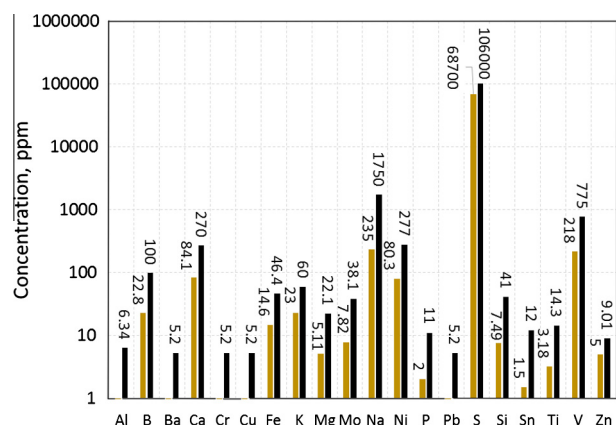
Fig. 2. The concentration of metals and sulfur present in the initial bitumen (yellow bars), and in n-pentane insoluble asphaltenes (black bars). (The y-axis is logarithmic). (For interpretation of the references to colour in this figure legend, the reader is referred to the web version of this article.)

discussion. It is well known that vanadium and nickel are present in the form of porphyrins [39]. However, very little is known about how other metals are linked to asphaltenes. One plausible explanation is that they are present in a colloidal form in the bulk of the original bitumen and then, during n-pentane treatment, they precipitated along with the n-pentane insoluble fraction of bitumen.

3.2. Summary of previously conducted experimental results

Table 1 below summarizes the performances of all experiments. No oil recovery was obtained from E5, as this experiment had to be terminated after 2.8 h due to plugging in production lines [28]. It has been determined that all produced oil samples contained both water and clay [30]. Both the cumulative produced oil amounts, including and excluding the clay and the water contents are summarized in Table 1. Details on separation of water and clays from produced oil samples are not in the scope of this study but can be found in previously published work [30]. The best performance in terms of oil recovery was obtained for E3 in which toluene (asphaltene soluble solvent) and n-hexane (asphaltene insoluble solvent) were coinjected with steam.

3.3. Extraction of residual oil from spent rock

The focus of this study is to investigate the pore-scale displacement mechanism for SAGD and Solvent-SAGD. Therefore, the residual oil saturation determination was carried out on spent rock samples collected at the end of each experiment from the regions

Table 1
Performance summary of SAGD and Solvent-SAGD experiments [26,28].

Experiment	Solvent used	Experimental time (h)	Produced oil recovery (oil + water + clay) (wt%)	Cumulative oil recovery (wt%)
E1	None	12	32.12[a]	10.20
E2	n-hexane	9	33.71[a]	23.47
E3	n-hexane + toluene	9	45.15[a]	24.52
E4	n-hexane or toluene with 1 h cycles	9	44.91[a]	20.84
E5	n-hexane + cyclohexane	2.8	0.00	0.00

[a] Produced oils are in the form of emulsions that contain water and clay [30].

given in Fig. 1. As previously mentioned, the postmortem samples from each experiment were divided into two zones; inside steam chamber region and outside steam chamber region (which is more representative of the steam chamber edge due to the experimental dimensions). Previously conducted contact angle measurements on the spent rock samples showed that the spent rock samples from all five experiments were showing oil-wet nature with slight differences in values [20]. Thus, we measured the amount of residual oil saturation, and we investigated the characteristics of residual oil to understand the reason behind the performance differences given in Table 1.

The residual oil samples were separated from the spent rock by using two strong solvents (S1 and S2) which effectively dissolve the heavier oil components and by implementing a thermal technique (Th). The TGA method (Th) was performed to conduct the thermal method on both spent rock and the original oil–sand mixture; a small amount of sample was combusted under isolation by the TGA device at a constant heating rate of 10 °C/min, and the weight loss at the temperature corresponding to complete decomposition of residual oil was used to calculate the residual oil amount. The initial oil sand mixture was prepared based on a fixed weight to maintain 84% bitumen saturation. Hence, the TGA experimental result of the initial oil sand mixture was used as a control experiment (black curve in Fig. A-1-B) to determine the thermal decomposition temperature of the bitumen in sand pack. Thus, the weight loss observed at around 585 °C (red dashed line in Fig. A-1) for all spent rock samples was used to determine the residual oil saturation. All residual oil saturation values determined through either solvent extraction or thermal decomposition, then, were normalized based on the constant sand pack volume, accordingly, Fig. 3 was constructed.

For the thermal method, lower residual oil saturation values were observed for inside steam chamber region. While the residual oil saturation values determined through thermal method are consistent with the literature definition of SAGD performance; lower inside steam chamber and higher at steam chamber edge [40]; solvent extraction methods show different trends for different experiments. Moreover, the FTIR analysis given in Fig. A-2, revealed significant clay presences at around 3600 cm^{-1} wavenumber region (this region is highlighted with arrows on Fig. A-2) [36]. The FTIR spectra will be further discussed in the following sections.

Therefore, the most reliable method to determine residual oil saturation is the thermal method (Th). The variations observed in
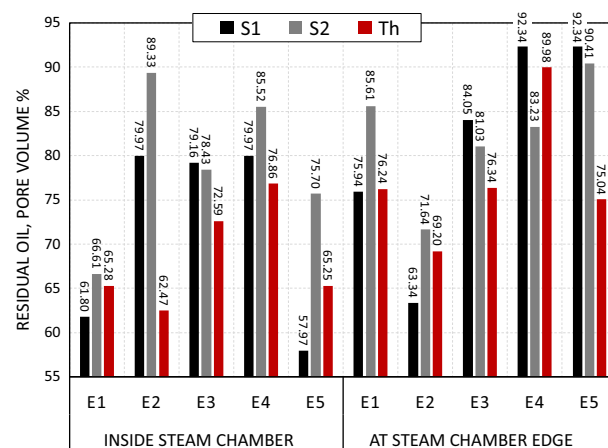

Fig. 3. Normalized residual oil saturation values based on two extraction methods; solvent [S1: mixture of 90% dichloromethane (DCM) and 10% methanol; S2: toluene] and thermal [Th: The thermal method by using Thermogravimetric Analyzer (TGA)]. Normalization was carried out by calculating the oil amount for constant rock weight.

solvent extraction methods are mainly due to asphaltene–clay interaction. The characteristics and the amount of the deposited asphaltenes are expected to be different from experiment to experiment and also to vary from the steam chamber to the steam chamber edge. Note that during solvent-SAGD experiments, n-hexane (asphaltene insoluble), toluene (asphaltene soluble), and cyclohexane (which has an intermediate solubility with asphaltenes) were tested, and the residual oil extraction was achieved by washing the spent rock sample either with DCM and methanol mixture (this mixture is asphaltene soluble) or toluene. Therefore, Fig. 3 shows the complex interactions of asphaltene solvents and non-solvents behavior with asphaltenes and with deasphalted oil.

In E1, in which steam is injected continuously for 12 h, the residual oil was measured lower for S1 than S2, this should be due to the interaction of solvents used during residual oil extraction with asphaltenes. The variation in solvent extraction results are due to the interaction of asphaltenes with clay, and the following section will discuss the amount of clay in residual oil samples. For E2, the residual oil saturation from solvent extraction shows very high values. Note that in this experiment, n-hexane was coinjected with steam for 9 h and n-hexane is insoluble in asphaltenes. Hence, it was expected to observe the higher amount of asphaltenes deposit for E2. Thus, the deposition of a higher amount of asphaltenes favored more clay-asphaltene interaction. In E3, an asphaltene solvent (toluene) and a non-solvent (n-hexane) were coinjected with steam for 9 h. Since less asphaltenes deposition was expected in E3, the less asphaltene–clay interaction was observed (Th values are close to S1 and S2 for E3). Because E4, in which toluene and n-hexane were cyclically injected, was ended with n-hexane cycle, the asphaltene deposition was expected higher than E3 and lower than E2, hence, in separated residual oil of E4, less asphaltene–clay interaction than E2 and more asphaltene–clay interaction than E3 were observed. In E5, no oil production was observed (Table 1), and the experiment had to be terminated by the end of 2.8-h experiment time. Therefore, for E5, the oil was displaced toward the steam chamber edge, but could not be produced. Thus, an increase in residual oil saturation was observed. Note that the sample location is critical for residual oil saturation determination, hence, the experiments have been repeated for validation.

3.4. Asphaltene solubility profile

During the separation of residual oil, two types of asphaltenes were removed from the spent rock together; precipitated asphaltenes and the movable asphaltenes in residual oil. The properties of precipitated asphaltenes can be different than movable asphaltenes. Because asphaltene solvents were used to extract residual oil, it is difficult to distinguish the precipitated asphaltenes from movable ones. Therefore, the asphaltene solubility profile tests were conducted on the bulk asphaltenes (precipitated + movable) separated from the residual oil. The stability parameter (ΔPS), which has been calculated by taking the integration of the asphaltene solubility profiles, was used to determine the stability of asphaltenes. The larger the stability parameter, the less stable the crude oil and the more polar the asphaltenes are (less soluble). In other words, the value of the higher stability parameter indicates a higher tendency of asphaltenes precipitation. The solubility profiles are summarized in Fig. A-3 and calculated ΔPS values are given in Table A-1.

Asphaltenes from inside the steam chamber region show more variability than those at the chamber edge indicating a larger effect of the solvents/steam in the steam chamber as expected [29]. In terms of variations that can be attributed to the use of different solvents, in both cases, inside and at the edge, the asphaltene solubility profile of the case E3 (SAGD with hexane + toluene) looks quite similar. This finding might indicate that conditions inside the steam chamber and the edge are similar to this particular blend. E4 (1 h [SAGD + Hexane (C6)] and 1 h [SAGD + Toluene]) results are similar to E1 (SAGD) results for inside the chamber regions. This result can be attributed to the use of toluene after hexane. It is well known that toluene is a strong solvent that solves asphaltenes, so, when it is injected after hexane, it can reverse any possible asphaltene precipitation induced by hexane. The net result is that E4 is similar to E1 (SAGD alone). It can also be noticed that in both cases, there is not a clear second peak in the plot (Fig. A-3). This finding is an indication that there was not preferential retention of the less soluble asphaltenes. In contrast, inside the chamber, the effects of E2 and E5 indicate that the asphaltenes that the preferentially precipitate are less soluble, as a clearly defined second peak shift to the right indicates. In the solubility profile method, the shift to the right of the signal indicates the presence of asphaltenes that are more difficult to dissolve in hydrocarbons. This phenomenon is the effect of using hexane as part of the injected blend of solvents. In the edge of the steam chamber, all the solubility profiles look pretty similar with the exception already discussed of E3.

3.5. Effect of oil components and clays on residual oil

The residual oil samples were divided into saturates, aromatics, resins, and asphaltenes (SARA) fractions to investigate further the impact of each fraction on pore-scale displacement. The ASTM D2007-11 standard method was followed for SARA analysis [31]. The original bitumen was reported to have 23.6 wt% saturates, 20 wt% aromatics, 21.9 wt% resins, and 34.6 wt% asphaltenes [30].

Because significant clay presence was observed in the residual oil samples and asphaltene fractions by FTIR analyses (Fig. A-2, the absorbance peaks observed around $3600 \, cm^{-1}$ wavenumber corresponds to the presence of clays [30]), the clay content of the residual oil samples was determined by solvent extraction and filtration (as described in Section 2). No water was detected in residual oil samples.

The experimental results (SARA and clay content of each residual oil sample) are given in the appendix part (Table A-1). The asphaltene content from inside steam chamber to at steam chamber edge could not yield a direct relation for different experiments. Thus, the mutual interaction of SARA fractions with clay content in the residual oil and in the residual oil asphaltenes were investigated with correlations and the correlations obtained from the experimental data are given in Fig. 4.

It is obvious that both resins to asphaltenes (RES/ASP) and asphaltenes to aromatics (ASP/ARO) ratios control the asphaltene–clay interaction. To clarify the interaction of clays with aromatic structures in bitumen, some control experiments were carried out under optical microscopy (Fig. 5).

Sand grains and clay particles are shown clearly in Fig. 5. First, the initial microscopic image of the sand–clay mixture (porous media used in the experiments-Fig. 5-A) was compared to the sand–clay mixture after water exposure (Fig. 5-B). In Fig. 5-B, the image at $100\times$ magnification shows noticeably the pore lining feature of clay after water interaction (darker areas around the sand grains are due to clay lining around sand grains). Then, the initial sand–clay mixture was exposed to the saturates fraction of original bitumen and a microscopic image was taken to observe the interaction of saturates with reservoir fines in pore-scale (Fig. 5-C). The sand grain has been highlighted on the image and the clay particles can be seen in small lumps in the pore space and on the sand grains. While the small clay-lump formation was observed, the interaction of those lumps with sand grains was not observed. The similar test was also done with aromatics (Fig. 5-D). It has been observed that clays formed clusters after interacted
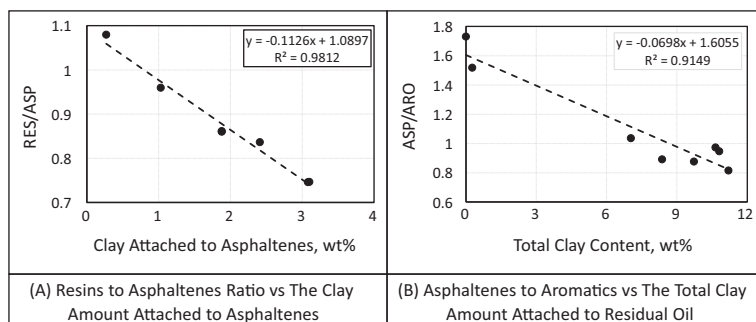
Fig. 4. (A) The correlation between Resins to Asphaltenes (RES/ASP) ratio and clay attached to asphaltenes. (B) The correlation between Asphaltenes to Aromatics (ASP/ARO) ratio and total clay content of the extracted residual oil. (Both correlations are obtained by 8 data points given in Table A-1. Two outliers are not changing the trend, however, changing the correlation equation).
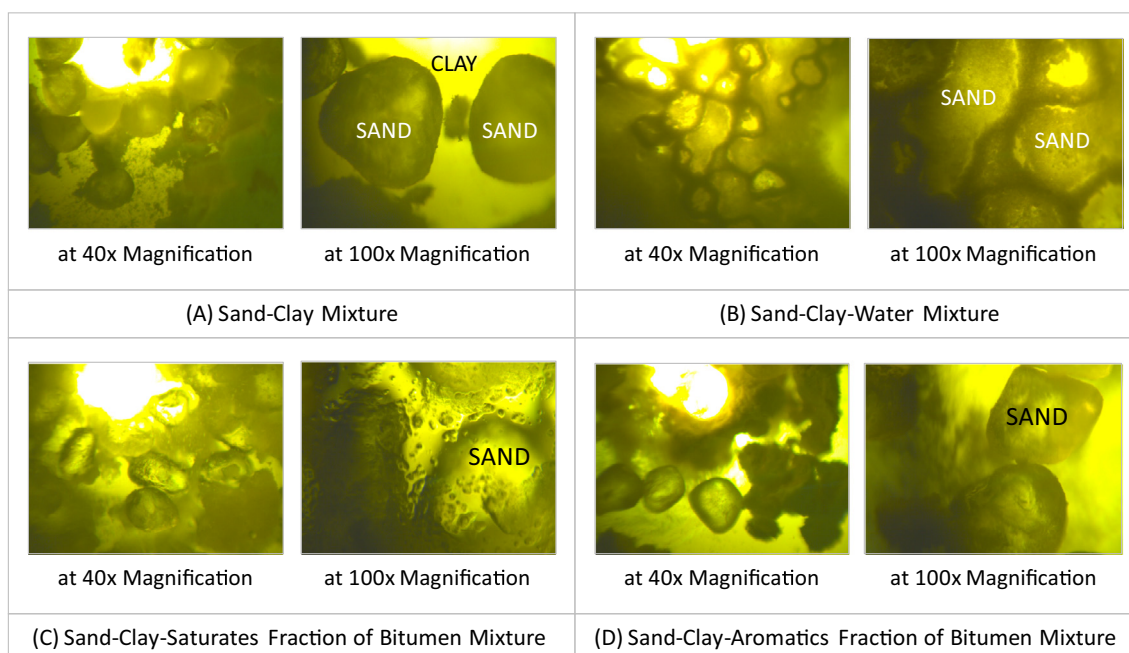

Fig. 5. Microscopic images of Sand–Clay mixture at 40× and 100× magnifications.
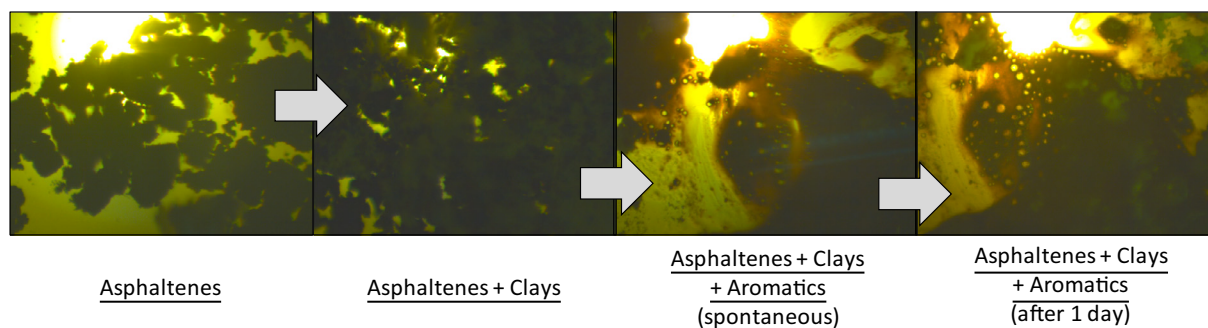

Fig. 6. Microscopic images at 40× magnification to observe spontaneous the interaction of asphaltenes with clays and the aromatics fraction of original bitumen.

with the aromatics fraction of bitumen. The interaction observed in Fig. 5-D explain the reason behind the correlation obtained in Fig. 4 better; clays are obviously interacting favorably with aromatics fraction. To support this finding, the control experiments have been extended, and similar analyses were achieved on asphaltenes fraction. Fig. 6 summarizes the asphaltenes–clays–aromatics interaction.

After adding one drop of aromatics fraction of bitumen on asphaltene–clay mixture (note that asphaltene–clay mixture was in solid-powder form initially), dissolution of asphaltenes was observed, and clays became invisible. However, after 1-day image (when partially the aromatics fraction was evaporated from the mixture) shows visible clay particles trapped in asphaltene clusters. Hence, the aromatics fraction of bitumen should be
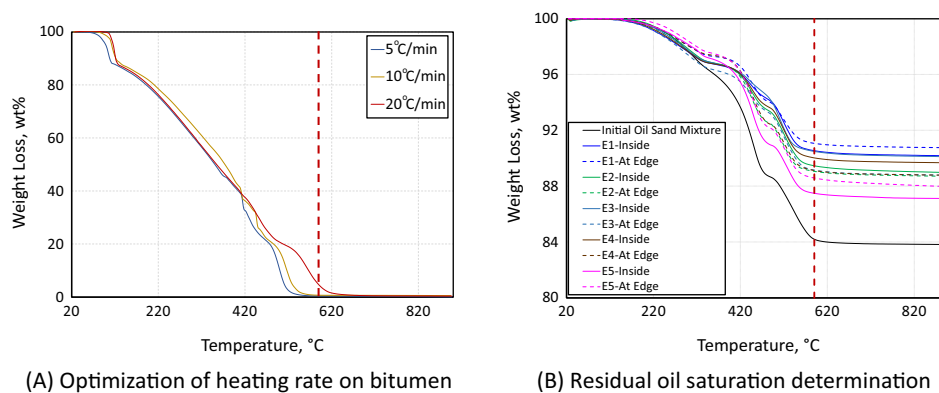
(A) Optimization of heating rate on bitumen

(B) Residual oil saturation determination

Fig. A-1. The experimental results of the TGA tests conducted at 10 °C/min heating rate.

(A) FTIR Spectra of Residual Oil Samples from Inside Steam Chamber Region

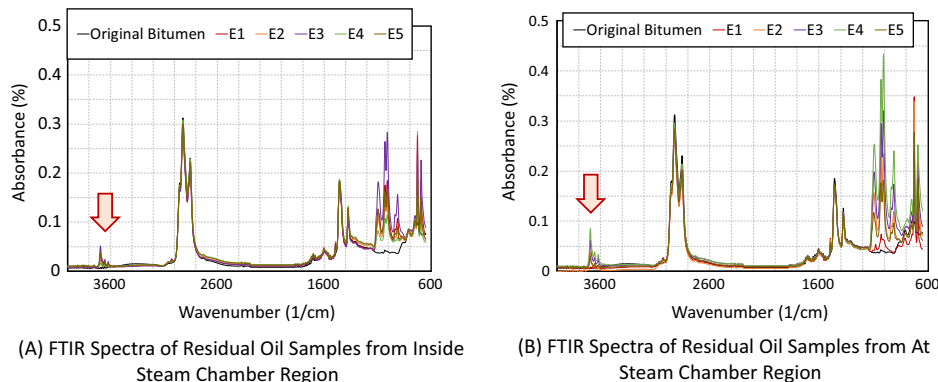(B) FTIR Spectra of Residual Oil Samples from At Steam Chamber Region

Fig. A-2. FTIR spectra of residual oil samples from (A) inside steam chamber and (B) at steam chamber edge regions (black curves are original bitumen sample FTIR).
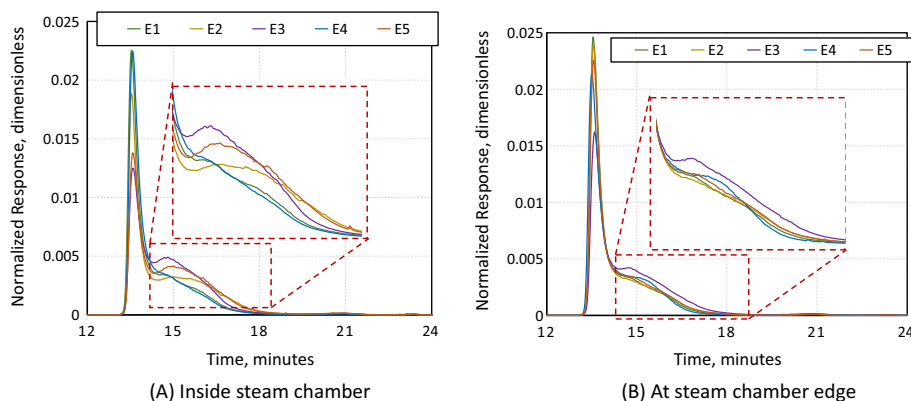

(A) Inside steam chamber

(B) At steam chamber edge

Fig. A-3. Asphaltene solubility profiles [33] for the extracted oils from inside and outside the steam chamber for E1: SAGD (Base Case), E2: SAGD + Hexane (C6), E3: SAGD + Hexane (C6) + Toluene, E4: 1 h [SAGD + Hexane (C6)] and 1 h [SAGD + Toluene], and E5: SAGD + Hexane (C6) + Cyclohexane.

responsible to enhance the asphaltene–clay interaction and most probably, asphaltene–clay interaction cannot be maintained without the presence of the aromatics fraction of crude oil. Thus, the residual oil saturation determination through solvent extraction could not provide reliable data. Note that in general, strong aromatic solvents are used to determine residual oil saturation, due to the interaction of aromatics with clay, the extracted oil cannot be free from clays.

Our results (combination of Figs. 4–6) suggest that the aromatics fraction of the residual oil is responsible for the transportation of clay lumps in asphaltenes, since aromatics are asphaltene soluble. The amounts of resins should be the main reason behind trapping of clay lumps in asphaltenes (Fig. 4-A). In other words, as the aromatics to asphaltenes ratio increases in residual oil, the total clay amount interacting with residual oil increases. Because aromatics are soluble in asphaltenes, clays are carried with aromatics and settled in asphaltenes, and then, the resins to asphaltenes ratio controls the clay trapping mechanism in asphaltenes. Moreover, as the resins to asphaltenes ratio decreases, the trapping of clays in asphaltenes increases (Fig. 4-A). And as the resins to asphaltenes ratio increases asphaltenes interact first with resins, if there is not sufficient amount of resins in residual oil to interact entire asphaltenes, then, the remaining asphaltenes interacts with clays. Still, this interaction becomes possible due to the transportation of clays with aromatics in asphaltenes. This feature of asphaltenes makes the residual oil saturation determination through solvent extraction misleading.

Table A1
Residual oil fractionation and the stability parameter of n-heptane insoluble asphaltenes.

Sample location	EXP#	Residual oil SARA fractions (wt%)				CLAYS (wt%)			ΔPS^a, dimensionless
		SAT[*]	ARO[*]	RES[*]	ASP[*]	IN ASP[*]	IN DAO[*]	TOTAL	
Inside steam chamber	E1	15.7	25.6	26.3	28.3	4.17	0	4.17	1.47
	E2	29	17	27.9	25.8	0.27	0	0.27	2.12
	E3	15.1	32.9	19.2	25.7	3.1	4.01	7.11	1.8
	E4	12.3	28.5	20.7	27.8	3.08	7.57	10.65	1.39
	E5	13.5	30.2	20.6	24.6	2.41	8.79	11.2	2.14
At steam chamber edge	E1	13.2	28.4	23.9	24.9	1.03	8.7	9.73	1.27
	E2	14.4	31.3	21.3	24.8	1.88	6.38	8.26	1.35
	E3	16.8	26	23.2	26.9	1.88	5.16	7.04	1.92
	E4	16.8	26.1	21.5	24.8	6.42	4.39	10.81	1.31
	E5	16.2	28.5	21.4	25.5	5.54	2.83	8.37	1.40

[*] SAT: Saturates; ARO: Aromatics; RES: Resins; ASP: Asphaltenes; DAO: deasphalted oil.
[a] The calculated stability parameter for n-heptane insoluble asphaltenes [20].

4. Conclusion

One SAGD and four Solvent-SAGD experiments were conducted previously. The residual oil saturations were determined to investigate the pore-scale displacement efficiency both for inside steam chamber region and at steam chamber edge regions. It has been found that the residual oil saturation determination through different solvent extraction methods provided different results. The SARA fractions and clay separations on residual oil samples revealed that asphaltene–clay interaction inhibits the proper separation of residual oil from reservoir rocks during solvent extraction methods. Further analysis showed that the asphaltene–clay interactions are controlled by the amount of resins and aromatics. As the aromatic content increases and/or resins content decreases, the asphaltene–clay interaction is enhanced. Since strong asphaltene solvents are used during solvent extraction methods, the asphaltene–clay interaction cannot be avoided during residual oil saturation determination through solvent extraction. Our results suggest that, the solvents used in any solvent extraction methods can provide valuable information on the behavior of asphaltenes in the bulk residual oil. However, the solvent extraction methods can be misleading due to the clay content of the residual oil. Thus, our results suggest that the use of thermal method for residual oil saturation determination produces the most accurate residual oil saturation values.

Appendix A

See Figs. A-1–A-3 and Table A1.

References

[1] Willhite GP. "Waterflooding" SPE Textbook Series 1986;3. ISBN: 978-1-55563-005-8.
[2] Green DW, Willhite GP. "Enhanced Oil Recovery" SPE Textbook Series 1998;6. ISBN: 978-1-55563-077-5.
[3] Chang MM, Maerefat NL, Tomutsa L, Honarpour MM. Evaluation and comparison of residual oil saturation determination techniques. SPE Form Eval 1988:251–62.
[4] Staub HL. Residual oil saturation determination, Wilmington Micellar-Polymer Project report no. DOE/BETC/1395-6, US DOE; 1983.
[5] Ward CE, Barnwell JL. Industrial survey of core handling, storage, and analysis procedures for ROS measurements, report no. DOE/BC/10022-6, US DOE; 1980.
[6] Presley CT. Sulfonate retention and residual oil saturation. SPE J 1983. 1983SPE-10343-PA.
[7] Rathmell JJ, Braun PH, Perkins TK. Reservoir waterflood residual oil saturation from laboratory tests. J Petrol Technol 1973;25(02):175–85.
[8] Yang P, Guo H, Yang D. Determination of residual oil distribution during waterflooding in tight oil formations with NMR relaxometry measurements. Energy Fuels 2013;27:5750–6.
[9] Sah SL. Encyclopaedia of Petroleum Science and Engineering, Kalpaz Publications, Delhi, p. 250.
[10] Treiber LE, Owens WW. A laboratory evaluation of the wettability of fifty oil-producing reservoirs. SPE J 1972;12(06). SPE-3526-PA.
[11] Prats M. Thermal recovery. SPE Monogr 1982;7.
[12] Anderson WG. Wettability literature survey- Part 1: rock/oil/brine interactions and the effects of core handling on wettability. J Petrol Technol 1986;38:1125–44.
[13] Swanson BF. Visualizing pores and nonwetting phase in porous rock. J Petrol Technol 1979;31(01). SPE-6857-PA.
[14] Raza SH, Treiber LE, Archer DL. Wettability of reservoir rocks and its evaluation. Prod Mon (United States) 1968;32(4).
[15] Hascakir B, Kovscek AR. Reservoir simulation of cyclic steam injection including the effects of temperature induced wettability alteration. SPE Western Regional Meeting, 27–29 may, Anaheim, California, USA. SPE-132608-MS; 2010.
[16] Combarnous M, Sourieau P. Les Methodes Thermiques de Production des Hydrocarbures. Revue Inst Francais du Petrole 1976:543–77. Chap. 3.
[17] Speight JG. The chemistry and technology of petroleum. 3rd ed. New York: Marcel Dekker; 1999. and references therein.
[18] Mullins OC. Review of the molecular structure and aggregation of asphaltenes and petroleomics. SPE J 2008;13(01). SPE-95801-PA.
[19] Amyx JW, Bass DM, Whiting RL. In: Petroleum reservoir engineering. McGraw Hill; 1960. p. 103–4. ISBN 07-001600-3.
[20] Kar T, Yeoh J, Ovalles C, Rogel E, Benson IP, Hascakir B. The impact of asphaltene precipitation and clay migration on wettability alteration for Steam Assisted Gravity Drainage (SAGD) and expanding Solvent-SAGD (ES-SAGD). In: SPE Heavy Oil Conference, 9–11 June, Calgary, Alberta, Canada. SPE-174439-MS; 2015.
[21] Dudley JW, Taberner C, LaMantia BC, Zhang E, McNett J. Rock-fluid interactions of a carbonate bitumen reservoir rock under steam-soak conditions-importance of testing under reservoir temperature and stree conditions. In: International Petroleum Technology Conference, 26–28 March, Beijing, China. IPTC-16802-MS; 2013.
[22] Mehrotra AK, Svrcek WY. Properties of cold lake bitumen saturated with pure gases and gas mixtures. Canad J Chem Eng 2009;66(4):656–65.
[23] Unal Y, Kar T, Mukhametshina A, Hascakir B. The impact of clay type on the asphaltene deposition during bitumen extraction with steam assisted gravity drainage. In: SPE International Symposium on Oilfield Chemistry 2015, 13–15 April 2015, Woodlands, Texas, USA, SPE-173795-MS; 2015.
[24] Butler RM, McNab GS, Lo HY. Theoretical studies on the gravity drainage of heavy oil during in-situ steam heating. In: 29th Canadian Chemical Engineering Conference, Sarnia, Ontario, Canada; 1979.
[25] Butler RM. A method for continuously producing viscous hydrocarbons by gravity drainage while injecting heated fluids. UK Pat. Appl GB 2,053,328; 1980.
[26] Mukhametshina A, Kar T, Hascakir B. Asphaltene precipitation during bitumen extraction with Expanding Solvent Steam Assisted Gravity Drainage (ES-SAGD): effects on pore-scale displacement. SPE J, SPE-170013-PA; 2015, in press. https://www.onepetro.org/journal-paper/SPE-170013-PA.
[27] Kar T, Williamson M, Hascakir B. The role of asphaltenes in emulsion formation for Steam Assisted Gravity Drainage (SAGD) and expanding Solvent SAGD (ES-SAGD). In: SPE Heavy and Extra Heavy Oil Conference-Latin America, 24–26 September, Medellin, Colombia. SPE-171076-MS; 2014.

[28] Mukhametshina A, Hascakir B. Bitumen extraction by expanding solvent-steam assisted gravity drainage (ES-SAGD) with asphaltene solvents and non-solvents. SPE 170013-MS; 2014.

[29] Nasr TN, Kimber KD, Vendrinsky, DA, Jha KN. Process enhancement in horizontal wells through the use of vertical drainage channels and hydrocarbon additives. In: SPE Western Regional Meeting, Society of Petroleum Engineers. SPE 21794-MS; 1991.

[30] Kar T, Hascakir B. The role of resins, asphaltenes, and water in water–oil emulsion breaking with microwave heating. Energy Fuels 2015;29(6):3684–90.

[31] Yang L, Wang J, Fan T, Buckley JS. Effect of crude oil composition on wettability of mica. In: International Symposium of the Society of Core Analysts, 21–24 September, Pau, France. SCA2003-01; 2003.

[32] Wiehe IA. Asphaltene solubility and fluid compatibility. Energy Fuels 2012;26:4004–16.

[33] Rogel E, Ovalles C, Moir M. Asphaltene stability in crude oils and petroleum materials by solubility profile analysis. Energy Fuels 2010;24(8):4369–74.

[34] ASTM. D2007-11: Standard test method for characteristic groups in rubber extender and processing oils and other petroleum-derived oils by the clay-gel absorption chromatographic method; 2011.

[35] ASTM. D6560-12: Standard test method for determination of asphaltenes (heptane insolubles) in crude petroleum and petroleum products; 2012.

[36] Kar T, Mukhametshina A, Unal Y, Hascakir B. The effect of clay type on steam assisted gravity drainage performance. J Canad Petrol Technol 2015;54 (6):412–23. SPE-173795-PA.

[37] Rogel E, Ovalles C, Moir ME, Schabron JF. Determination of asphaltenes in crude oil and petroleum products by the on column precipitation method. Energy Fuels 2009;23(9):4515–21.

[38] Kaminski TJ, Fogler HS, Wolf N, Wattana P, Mairal A. Classification of asphaltenes via fractionation and the effect of heteroatom content on dissolution kinetics. Energy Fuels 2000;14(1):25–30.

[39] Podobaeva TP, Gonsales MG, Polyakova AA, Kogan LO, Vasilenko GV. Determination of metal porphyrins in asphaltenes. Chem Technol Fuels Oils 1980(5-6):351–3.

[40] Butler RM. SAGD comes of Age! J Canad Petrol Technol 1998;37(07). PETSOC-98-07-DA.